Canadian RCM Projected Changes to Extreme Precipitation Characteristics over Canada

B. MLADJIC AND L. SUSHAMA

Centre Étude et Simulation du Climat à l'Échelle Régionale, University of Quebec at Montreal, Montreal, Quebec, Canada

M. N. KHALIQ

Adaptation and Impacts Research Section, Climate Research Division, Environment Canada, Montreal, Quebec, Canada

R. LAPRISE

Centre Étude et Simulation du Climat à l'Échelle Régionale, University of Quebec at Montreal, Montreal, Quebec, Canada

D. CAYA

Centre Étude et Simulation du Climat à l'Échelle Régionale, University of Quebec at Montreal, and Ouranos, Montreal, Quebec, Canada

R. ROY

Ouranos, Montreal, and Hydro-Quebec, Varennes, Quebec, Canada

(Manuscript received 8 July 2010, in final form 28 November 2010)

ABSTRACT

Changes to the intensity and frequency of hydroclimatic extremes can have significant impacts on sectors associated with water resources, and therefore it is relevant to assess their vulnerabilities in a changing climate. This study focuses on the assessment of projected changes to selected return levels of 1-, 2-, 3-, 5-, 7- and 10-day annual (April–September) maximum precipitation amounts, over Canada, using an ensemble of five 30-yr integrations each for current reference (1961–90) and future (2040–71) periods performed with the Canadian Regional Climate Model (CRCM); the future simulations correspond to the A2 Special Report on Emissions Scenarios (SRES) scenario. Two methods, the regional frequency analysis (RFA), which operates at the scale of statistically homogenous units of predefined climatic regions, with the possibility of downscaling to gridcell level, and the individual gridbox analysis (GBA), are used in this study, with the time-slice stationarity assumption. Validation of model simulated 20-, 50- and 100-yr return levels of single- and multiday precipitation extremes against those observed for the 1961–90 period using both the RFA and GBA methods suggest an underestimation of extreme events by the CRCM over most of Canada. The CRCM projected changes, realized with the RFA method at regional scale, to selected return levels for the future (2041–70) period, in comparison to the reference (1961–90) period, suggest statistically significant increases in event magnitudes for 7 out of 10 studied climatic regions. Though the results of the RFA and GBA methods at gridcell level suggest positive changes to studied return levels for most parts of Canada, the results corresponding to the 20-yr return period for the two methods agree better, while the agreement abates with increasing return periods, that is, 50 and 100 yr. It is expected that the increase in return levels of short and longer duration precipitation extremes will have severe implications for various water resource–related development and management activities.

1. Introduction

Extreme hydroclimatic events such as precipitation extremes, floods, and droughts can impact society significantly, bringing enormous environmental, social, and political repercussions. It is therefore important to

Corresponding author address: L. Sushama, Centre Étude et Simulation du Climat à l'Échelle Régionale, University of Quebec at Montreal, 201-President-Kennedy, Montreal, QC H3C 3P8, Canada.
E-mail: sushama.laxmi@uqam.ca

DOI: 10.1175/2010JCLI3937.1

investigate changes to characteristics of these extreme events in the context of a changing climate. Assessment of changes to characteristics of precipitation extremes due to variations in greenhouse gas concentrations was investigated in previous studies using global climate model (GCM) simulations (e.g., Zwiers and Kharin 1998; Kharin and Zwiers 2000; Palmer and Räisänen 2002; Voss et al. 2002; Kiktev et al. 2003, 2004; Wehner 2004) as well as using regional climate model (RCM) simulations—for example, Fowler et al. (2005) and Ekström et al. (2005) for the United Kingdom; Booij (2002) for northwestern Europe; Semmler and Jacob (2004), Frei et al. (2006), Beniston et al. (2007), and May (2008) for the whole of Europe; and Mailhot et al. (2007) for southern parts of the Quebec province of Canada. In the case of GCMs, coarse spatial resolution poses limitations to the simulation of mesoscale processes and to the representation of topographic features, and hence the projected changes derived using the GCM simulations are considered with some reservations for water-related impact and adaptation studies. RCMs, with their higher spatial resolution, compared to that of the GCMs, allow for greater topographic realism and finer-scale atmospheric dynamics to be simulated and thereby represent a possibly more adequate tool for reproducing the processes involved in the formation of precipitation and therefore to generate information required for many regional impact and adaptation studies. Also, RCMs were found to reproduce the main characteristics of the larger-scale hydroclimate during episodes of extreme precipitation (Anderson et al. 2003) and prominent patterns of precipitation extremes on scales not resolved by GCMs (Frei et al. 2003; Fowler et al. 2005).

In general, extreme values are described in terms of return levels or quantiles. These are the values that are exceeded, on average, once every specified number of years, commonly known as return period. Return levels are generally computed by fitting a parametric distribution to a sample of annual maximum (AM) or peaks-over-threshold (POT) values. In the former method (AM), which is very commonly used because of its simple structure, only one value from each year/season is considered. For the latter method (POT), more than one value per year/season could be considered. Since extreme events are rare and historical records are often short, estimation of frequencies of extreme events is challenging. The above is still true for climate model simulations because the models are generally run for 30-yr time slices in current and future periods. This limitation of longer records, whether observed or modeled, can be overcome by using a regional frequency analysis (RFA; Hosking and Wallis 1997), which trades space for time by pooling observations from different sites (gridboxes) in a given homogeneous region to compensate short records at individual sites (gridboxes) within the region. This method has been successfully used by Fowler et al. (2005) and Ekström et al. (2005) with the Hadley Centre Regional Climate Model (HadRM3H) for developing future projections of changes in extreme rainfalls over the United Kingdom. The other approach commonly used is the gridbox analysis (GBA), which is based on individual gridcells of the climate model (e.g., Fowler et al. 2005 and Ekström et al. 2005). While RFA has the advantage of providing higher reliability for return levels associated with larger return periods, GBA provides more spatial detail, as the analysis is performed for each gridbox. Thus, both approaches complement each other.

This study focuses on the evaluation and assessment of future changes to selected return levels of single and multiday (i.e., 1-, 2-, 3-, 5-, 7-, and 10-day) AM precipitation amounts, for the April–September period over Canada, using an ensemble of Canadian RCM (CRCM) integrations following the RFA and GBA approaches. It should be recognized that there is currently no comprehensive high-resolution observed dataset of precipitation that would allow a satisfactory evaluation of the CRCM with respect to its representation of precipitation extremes. The best dataset available for the region is from Environment Canada, described later in the article, and is used to evaluate the CRCM performance in this study.

The paper is organized as follows. A brief description of the CRCM and the simulations used in the analysis are given in section 2. Description of the Canadian climatic regions, which are used to develop the RFA approach, along with details of the observational records, which are used to validate the CRCM, is provided in section 3. Section 4 describes the methodology used, while section 5 shows results related to CRCM validation and projected changes to precipitation extremes. This is followed by the discussion and main conclusions of the study in section 6.

2. Model and simulations

The model used in this study is the latest operational version of the CRCM, that is, the fourth generation of the CRCM. A detailed description of the earlier versions of the CRCM can be found in Caya and Laprise (1999) and later modifications in Laprise et al. (2003) and Sushama et al. (2010). The current operational version of the CRCM uses the Canadian Land Surface Scheme (CLASS), version 2.7 (Verseghy et al. 1993). The CRCM's horizontal grid is uniform in polar stereographic projection, and its vertical resolution is variable with a Gal-Chen scaled-height terrain following coordinate. In the most recent version, subgrid-scale physical

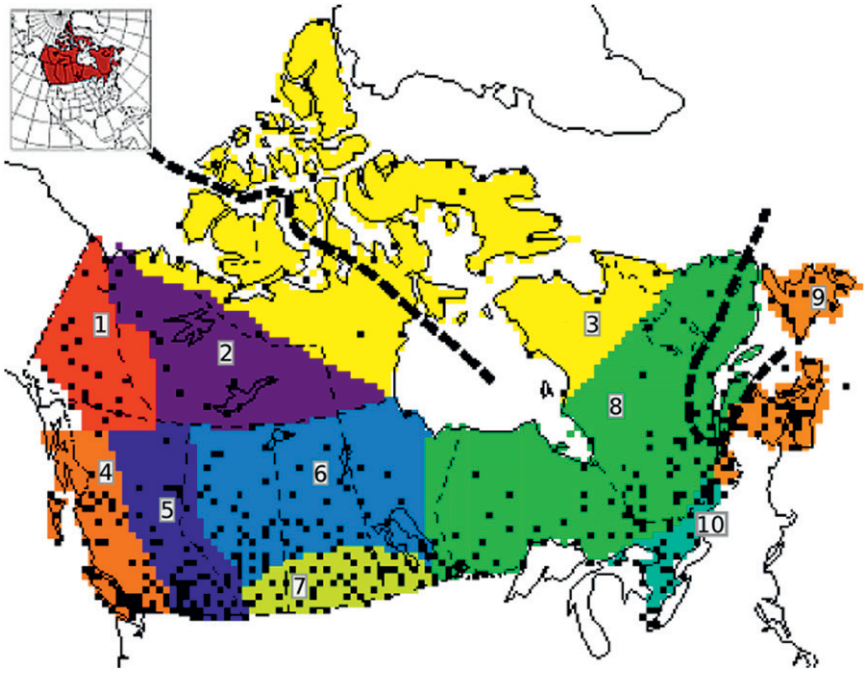

FIG. 1. Canadian climatic regions: 1) YUKON, 2) MACK, 3) EARCT, 4) WCOAST, 5) WCRDRA, 6) NWFOR, 7) NPLAINS, 8) NEFOR, 9) MRTMS, and 10) GRTLKS. Each of the EARCT and NEFOR regions are divided into two subregions, that is, EARCT1 and EARCT2 and NEFOR1 and NEFOR2. These divisions are shown by dashed lines; the region north (south) of the dashed line is EARCT1 (EARCT2), while NEFOR1 (NEFOR2) is the part of NEFOR to the west (east) of the dashed line. Spatial distribution of the CRCM gridcells (black squares), where at least one observation station is found, is also shown. Computational domain of the CRCM is given in the inset.

parameterization follows the Canadian General Circulation Model Version III (CGCM3) package (Scinocca and McFarlane 2004; McFarlane et al. 2005), with the exception of the cumulus parameterization that follows the formulation of Kain and Fritsch (1990) as modified by Bechtold et al. (2001).

An ensemble of 10 30-yr CRCM integrations are considered in this study, of which five correspond to the current reference (1961–90) period and the other five are the corresponding simulations for the future (2041–70) period. The five CRCM pairs perform dynamical downscaling of five different members of an ensemble of CGCM3 simulations to produce climate projections at regional scale following the twentieth-century climate (20C3M) scenario (Houghton et al. 2001) for the current reference period and Special Report on Emissions Scenarios (SRES) A2 scenario (Houghton et al. 2001) for the future period; it should be noted that the five driving CGCM3 members were initiated in 1850 with different initial conditions. The five CGCM3 driven simulations for 1961–90 will be referred to as ''reference simulations'' and noted R1, R2, R3, R4, and R5, while corresponding simulations for 2041–70 will be referred to as ''future simulations'' and noted F1, F2, F3, F4, and F5 in this paper. In addition to the above simulations, a validation run spanning the 1961–90 period, where the CRCM is driven by the 40-yr European Centre for Medium-Range Weather Forecasts (ECMWF) Re-Analysis (ERA-40; Uppala et al. 2005) is also considered and will be referred to as ''validation simulation'' (VS). All CRCM simulations are performed at a horizontal resolution of 45 km true at 60°N over a North American domain shown in the inset in Fig. 1.

3. Description of Canadian climatic regions and observational records

a. Climatic regions

The RFA approach based on *L* moments (Hosking and Wallis 1997) used in this study involves regional pooling of data over regions that are considered statistically homogeneous. Identification of such homogeneous regions over the study area is usually the first and the most difficult task in RFA as it may involve many subjective decisions (GREHYS 1996). In this study, previously defined

Canadian climatic regions from Plummer et al. (2006), shown in Fig. 1, are adopted as the basis for developing RFA approach. The climatic regions are as follows: Yukon Territory (YUKON), Mackenzie Valley (MACK), and East Arctic (EARCT) in the north; West Coast (WCOAST), Western Cordillera (WCRDRA), Northwest Forest (NWFOR), and Northern Plains (NPLNS), distributed along the western and prairie regions of Canada; and the Northeast Forest (NEFOR), Great Lakes (GRTLKS), and Canadian Maritimes (MRTMS) on the eastern part of Canada. It should be noted that though the original definition of WCOAST, WCRDRA, NPLNS, and GRTLKS regions are spread over the Canadian and the U.S. territory, but this study focuses only on Canada.

b. *Observational records*

Observational records used in this study consist of 495 stations included in the Canadian rehabilitated precipitation dataset (Mekis and Hogg 1999) of Environment Canada. This dataset was developed by applying adjustments for known reasons of nonhomogeneity, for example, changes in instrument type, station relocations, trace biases, etc. (Vincent and Mekis 2009). Most of the records are available until 2007 and for some stations records go as far back as 1900. Spatial distribution of the CRCM gridcells containing at least one station is shown in Fig. 1. It is clear from this figure that most of the stations are concentrated in the southern parts of the country, along the border with the United States. Central, east-central, and northern regions have a significantly less dense network of stations. This is an obvious limitation of the rehabilitated precipitation dataset. This dataset is used for verifying statistical homogeneity of the Canadian climatic regions in current climate, discussed in the earlier section, and for selecting the most appropriate regional distribution for modeling observed 1-, 2-, 3-, 5-, 7-, and 10-day AM precipitation amounts for the 1961–90 April–September period, in an RFA setting described in detail in the section to follow. In addition, this dataset is used in the validation of CRCM-simulated extremes for both RFA and GBA approaches. The April–September period is chosen to minimize mixing of snow and rainfall extremes or, in other words, to maintain homogeneity of the samples of precipitation extremes. As the reliability of the analyses is highly dependent on the quality as well as on the completeness of records, a year with more than five missing daily values is considered a missing year and only those stations having at least 70% valid years (i.e., 21 out of 30 years) are considered for the analyses. The total number of available stations and those retained for analysis following the missing value and station inclusion criteria (given in parentheses) are 21 (15) for YUKON, 16 (9) for MACK, 39 (33) for EARCT, 66 (58) for WCOAST, 65 (59) for WCRDRA, 58 (53) for NWFOR, 46 (43) for NPLNS, 86 (73) for NEFOR, 63 (59) for MRTMS, and 35 (30) for GRTLKS regions. In total, the number of stations considered in this study is 432 out of 495.

4. Methodology

As discussed earlier, two complementary methods are used to assess the CRCM performance and projected changes to selected return levels of precipitation extremes over Canada: the RFA and the GBA. For the application of these two methods it is assumed that the distribution of extremes remain stationary for the periods 1961–90 and 2041–70. Analyses are performed using 1-, 2-, 3-, 5-, 7-, and 10-day observed and simulated AM precipitation amounts, which are obtained using a moving window approach. To begin with, the CRCM ''performance errors'' due to the internal dynamics and physics of the model and ''boundary forcing errors'' due to the errors present in the driving data (Sushama et al. 2006) are assessed by comparing observed return levels with those from the validation simulation and the return levels from the validation and reference simulations, respectively, for both RFA and GBA approaches. Assessment of the performance and boundary forcing errors of CRCM is followed by an analysis of the CRCM reference and future period integrations, to assess projected changes to characteristics of single- and multiday precipitation extremes over Canada. The GBA and RFA approaches are discussed in detail below.

a. *L-moments-based RFA approach*

In general, there are two main steps involved in a RFA approach: 1) identification of suitable statistical homogeneous regions and 2) selection of an appropriate regional distribution to generate regional growth curves, where a regional growth curve represents a dimensionless relationship between frequency and magnitude of extreme values. In implementing these two steps, samples of precipitation extremes derived from the above-discussed dataset are used.

For verifying statistical homogeneity of Canadian climatic regions and their subdivision into smaller homogeneous regions, regional homogeneity tests based on L-moment ratios devised by Hosking and Wallis (1997) are used. According to these authors, heterogeneity measures for a region are based on values of H_1, H_2, and H_3, where H_1, H_2, and H_3 are weighted standard deviation of (i) L coefficient of variation, (ii) L skewness, and (iii) L kurtosis, respectively; H_1, H_2, and H_3 are derived using Monte Carlo simulations. A region may be regarded

as ''acceptably'' homogenous for H values below 1, ''possibly'' heterogeneous for H values between 1 and 2, and ''definitely'' heterogeneous for H values equal and above 2. For regions with H values greater than 2, a further subdivision into smaller regions is undertaken with the objective of improving on return-level estimates. This subdivision is undertaken using the cluster analysis algorithm (Hosking and Wallis 1997) if this algorithm resulted in meaningful contiguous subdivisions.

Once the statistical homogeneous regions have been identified, the next step is the selection of an appropriate regional distribution from among few candidate distributions for developing regional growth curves. The candidate distributions considered in this study include Generalized Extreme Value (GEV), Generalized Pareto (GPA), Generalized Logistic (GLO), Pearson-Type 3 (PE3), and Generalized Normal (GNO); cumulative distribution functions and L-moment relationships for these distributions can be found in Hosking and Wallis (1997). For a single site or a single gridcell, parameter estimation for any candidate distribution is performed by equating sample L moments (more preferably their ratios) to their theoretical values and solving the resulting equations directly or through iterative numerical algorithms. For the RFA approach, sample size–weighted averaged values of L-moment ratios are used for parameter estimation of the candidate regional distributions.

The Z test developed by Hosking and Wallis (1997) is used to pick the most appropriate regional distribution from among the candidate distributions GEV, GPA, GLO, PE3, and GNO. The distribution with the smallest value of the Z-test statistic is chosen as the best candidate distribution. It should be noted that the same distribution type is used for the analysis of extremes derived from the validation, reference, and future period integrations. This approach is followed to maintain distributional consistencies under the assumption that a three-parameter distribution is sufficiently flexible to describe changes in distributional characteristics that would occur between observations and validation simulation, as well as between reference and future period integrations.

After selection of an appropriate regional distribution for each statistically homogeneous region, comparisons of selected return levels of 1-, 2-, 3-, 5-, 7-, and 10-day precipitation extremes, obtained from observations and validation simulation of the model and validation and reference simulations of the model for the period 1961–90, are carried out to assess CRCM performance and boundary forcing errors, respectively. The selected return periods considered in this study are 20, 50, and 100 yr. The at-site (gridcell) return levels of the abovementioned single- and multiday precipitation extremes are computed by multiplying growth factors, derived from regional growth curves fitted to observed (CRCM simulated) extremes, for studied return periods, with respective at-site (gridcell) mean values of extremes. At-site refers to observation station location.

Validation of CRCM simulated extremes is followed by an assessment of projected changes to return levels of single- and multiday precipitation extremes in an RFA setting at both regional and gridcell level. As pointed out earlier, the best-fitting regional distribution selected for observed extremes is used in the analysis of extremes for both reference (R1–R5) and future (F1–F5) period integrations, but by reestimating its parameters for each case studied.

For developing projected changes, gridcell return levels are computed as discussed earlier, except that ensemble average of growth factors and gridcell mean values of extremes are considered. Similarly, regional return values are computed by multiplying ensemble average of regional growth factors, derived from regional growth curves, with the ensemble mean of regionally averaged gridcell mean values of extremes.

Uncertainty associated with the projected regional changes to return levels of single- and multiday precipitation extremes are assessed using the nonparametric vector bootstrap resampling method (Efron and Tibshirani 1993; GREHYS 1996; Davison and Hinkley 1997; Khaliq et al. 2009). This method is used as it takes care of the influence of first-order spatial correlations on estimates of uncertainty, which is expressed in the form of a confidence interval for any given return level. In the RFA approach considered here, this relates to the range of values in which the regional growth curves can be expected to lie. Therefore, an estimate of uncertainty in the regional growth curves for the reference (R1–R5) and future (F1–F5) simulations is carried out. For each studied region, $B = 1000$ resamples for each of the ensemble members are used to develop confidence intervals using two different approaches: 1) the standard error–based approach (Cunnane 1989; Hall et al. 2004) and (2) the test-inversion approach (Carpenter 1999; Faulkner and Jones 1999; Burn 2003). Let y^T be the T-yr regional growth factor for either of the R1–R5/F1–F5 simulations, and y_i^T the corresponding T-yr regional growth factor for the ith resample. For the first approach, an estimate of the bootstrap standard deviation of y_i^T values, commonly referred to as standard error of y^T [i.e., SE(y^T)], is obtained and confidence intervals are estimated using the Gaussian assumption, that is, by assuming that y^T is normally distributed. According to this approach, a 95% confidence interval is given by $[y^T \pm 1.96 \times \mathrm{SE}(y^T)]$. This method results in symmetric intervals. These intervals are multiplied by the regionally averaged mean value of the respective ensemble member

extremes to obtain an estimate of uncertainty. If for a given pair, for example, R1 and F1, the confidence intervals do not overlap, it indicates that the projected change from reference to future climate conditions is statistically significant.

For implementing the second approach, bootstrap residuals, $e_i = y_i^T - y^T$, for either of the R1–R5/F1–F5 simulations, are ranked in ascending order to obtain $m = (\alpha/2)(B + 1)$ and $p = (1 - \alpha/2)(B + 1)$ percentile values, where α is the significance level. For a $(1 - \alpha)\%$ confidence interval, this means choosing the mth and pth e_i values and obtaining the confidence interval as $(y^T - e_p, y^T - e_m)$. These intervals are multiplied by the regionally averaged mean value of the respective ensemble member extremes to obtain an estimate of uncertainty. Unlike the first approach, the second approach often may lead to asymmetric confidence intervals.

b. GBA approach

For this approach, a frequency analysis is performed by considering each CRCM gridcell as an independent entity. Distribution fitting analysis and selection of the best-fitting distribution for each gridcell can be performed in a similar manner as for the RFA approach described above. However, this analysis can only be performed for those gridcells where an observation station is found. For the remaining gridcells, one has to subjectively assume a suitable distribution. We therefore use the overall best-fit distribution, found after implementing the RFA approach, for implementing the GBA approach for the entire study area. Thus, for all gridcells, the type of the distribution stays the same for both reference and future period integrations. As in the case of RFA, both validation and assessment of projected changes are performed using this approach.

5. Results

Since statistical homogeneity of Canadian climatic regions is a prerequisite for the RFA approach, results from this analysis are presented first, followed by CRCM evaluation and projected changes. Though complete analyses are performed for 1-, 2-, 3-, 5-, 7-, and 10-day precipitation extremes, detailed results are presented only for 1-, 3-, and 7-day extremes. Where appropriate, results for the remaining (i.e., 2-, 5-, and 10-day) extremes are also discussed.

a. Statistical homogeneity analysis of Canadian climatic regions

Statistical homogeneity of each of the predefined climatic regions, adopted from the work of Plummer et al. (2006), is examined, with the available number of stations that satisfy the station inclusion criteria described earlier in the section on methodology for 1-, 2-, 3-, 5-, 7-, and 10-day observed precipitation extreme cases. If the calculated values of the H statistics are higher than 2 for at least three out of six cases (e.g., if H statistics are simultaneously higher than 2 for 1-, 3-, and 7-day precipitation extremes) then further subdivision of the region is undertaken, conditional to a successful implementation of the cluster analysis algorithm. Seven predefined regions (YUKON, MACK, WCOAST, NWFOR, NPLNS, GRTLKS, and MRTMS) pass this criterion, while the remaining WCRDRA, EARCT, and NEFOR regions do not, and hence their subdivision into smaller homogeneous subregions is attempted using cluster analysis. Satisfactory clustering was achieved for EARCT and NEFOR regions only. Hence, EARCT region is subdivided into EARCT1 and EARCT2 (shown in Fig. 1 using a dashed line) and NEFOR into NEFOR1 and NEFOR2 (also shown in Fig. 1). It was not possible to subdivide the WCRDRA region into smaller contiguous homogeneous regions, and hence this region was considered as is, despite its doubtful homogeneity; perhaps it may have been possible to subdivide this region into smaller noncontiguous homogeneous regions, but such a subdivision was not considered since the focus of this study was to find contiguous smaller homogeneous regions within the predefined larger climatic regions of Plummer et al. (2006). Based on the analyses presented and discussed above, a set of 12 climatic regions (shown in Fig. 1) is considered for RFA of AM values of single- and multiday precipitation events.

b. Validation of CRCM simulations

Observed regional growth curves are compared to those developed from model simulated (VS) extremes in Fig. 2, using Gumbel plots, for six selected regions: YUKON, WCOAST, MRTMS, GRTLKS, NWFOR, and EARCT2. These regions were chosen such that they represent the western, eastern, southern, interior, and northern parts of Canada. The shapes of growth curves for these six regions also represent the variety of shapes noted for the remaining six regions. The growth curves for each region are developed using the best-fitting distribution (shown on each subplot of Fig. 2) found on the basis of a Z test (Hosking and Wallis 1997). Many of the observed growth curves tend to follow a straight line, suggesting a light upper tail. However, the curves for GRTLKS, MRTMS, MACK, EARCT1, and NEFOR2 (figures not shown for the latter three regions) regions exhibit slight upward curvature, suggesting that distributions could be slightly heavy tailed. This behavior is particularly evident for 1-day precipitation extremes for GRTLKS. The heavy tailed behavior could be due to

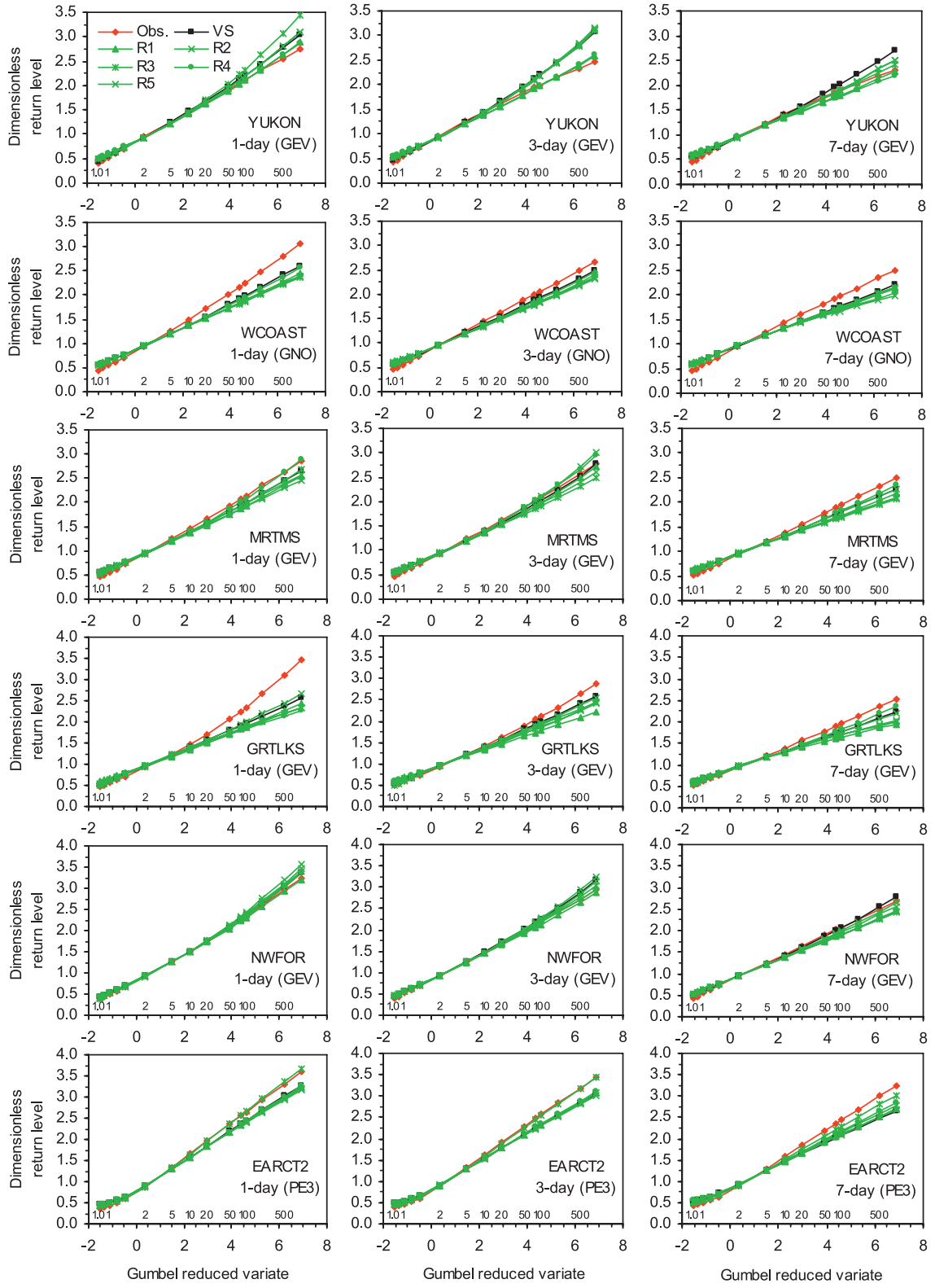

FIG. 2. Comparison of regional growth curves for 1-, 3-, and 7-day annual (April–September) maximum precipitation amounts, derived from the observed data, CRCM validation simulation (VS) and reference (R1–R5) simulations, for six selected regions. The plots are developed on Gumbel probability paper, wherein the inner scale along the x axis shows return periods. The best-fitting regional distribution is indicated in each panel.

extremes associated with convective activity, which is usually responsible for heavy downpours during the summer (June–August) months. Compared to observed growth curves, those for the validation simulation generally exhibit light tail behavior, suggesting that the extreme upper tail is underrepresented by the model. However, some exceptions can be noticed, for example, YUKON and NWFOR for single- and multiday precipitation extremes.

After comparing shapes of the regional growth curves, a direct comparison of 20-, 50-, and 100-yr return levels is carried out and results for the same six regions, as mentioned above, are shown in Fig. 3. Since the maximum length of individual samples included in the analysis is just 30 yr, we assume that 1 in 100-yr frequency is a reasonable upper limit for extrapolation; beyond this level, it would be difficult to place any confidence on the extrapolated values. In general, model underestimates return levels leading to negative performance errors, except for YUKON where positive performance errors are noted. Results also suggest that for WCOAST and WCRDRA regions, model-simulated values agree better with those observed for lower return levels. It is important to mention here that gridcell-based precipitation of GCMs and RCMs have the spatial characteristics of areal averages, and hence average precipitation for an area will in general be less than the precipitation estimated at a point (e.g., Osborn and Hulme 1997). This effect is expected to be stronger for heavy events as the spatial dimensions of precipitation events tend to decrease as the intensity increases. To address this issue, areal reduction factors (ARFs) can be used to relate the point precipitation with the areal average precipitation. However, there is no clear understanding and consensus on how this relationship should be developed for grid-cell-based precipitation simulated by regional and global climate models. Because of this uncertainty, we do not attempt to apply any empirically derived ARF to convert point precipitation into areal average precipitation.

Estimation of the boundary forcing errors (i.e., the influence of errors in the driving CGCM3 simulations) on simulated precipitation extremes can be achieved by comparing regional growth curves for the validation and reference simulations, for all regions. These growth curves for the selected six regions are also shown in Fig. 2. The growth curves corresponding to the reference simulations are similar to that of the validation simulation for the majority of the regions. However, differences between the validation and reference simulation growth curves can be noticed in the extreme upper tails for some regions, for example, YUKON and MRTMS. This suggests that the effect of boundary forcing data on the shapes of the growth curves is important for some regions, particularly for larger return levels. The spread among the members (R1–R5) is particularly large for higher return periods. Nevertheless, in general, the members demonstrate very similar behavior. The 20-, 50-, and 100-yr return levels for R1–R5 simulations for the six regions are shown in Fig. 4, where these return levels are plotted against the ones obtained from the validation simulation. For some regions [e.g. MRTMS, NWFOR, and NPLNS (figure not shown)], the points scatter along the line of perfect match, while for others (e.g., GRTLKS and YUKON) the points fall below this line suggesting negative boundary forcing errors. For 20-, 50-, and 100-yr return levels of 1-day (7-day) precipitation extremes, average boundary forcing errors are −19% (−22%) for YUKON; −16% (−10%) for MACK; −13% (−16%) for EARCT1; −10% (−10%) for EARCT2; −5% (−2%) for WCOAST; 0% (−4%) for WCRDRA; −3% (−5%) for NWFOR; 2% (−6%) for NPLNS; −10% (−13%) for NEFOR1; −6% (−8%) for NEFOR2; −2% (−2%) for MRTMS; and −11% (−3%) for GRTLKS regions. In general, the boundary forcing errors are smaller in magnitude compared to the performance errors.

Similar assessment of CRCM performance and boundary forcing errors are also carried out for the GBA approach. In this approach, the GEV distribution is fitted by the method of L moments to samples of single- and multiday observed precipitation extremes, derived from daily precipitation time series obtained by averaging the daily precipitation values recorded at stations that fall within each gridcell. The overall characteristics of the performance and boundary forcing errors for the GBA (figure not shown) are similar to those for the RFA, for the various studied regions. As for the RFA approach, the boundary forcing errors are smaller in magnitude compared to the performance errors.

c. *Projected changes to precipitation extremes*

1) RFA APPROACH

Projected changes to precipitation extremes are studied at the regional and gridcell scales. As discussed earlier, the same best-fit regional distribution that is used in the validation/reference simulations is used for the future simulations. For brevity, the plots of future regional growth curves are not shown. The projected changes at regional level will be presented first followed by those at gridcell level.

(i) Regional-level projections

Figure 5 shows 20-, 50-, and 100-yr return levels for 1-, 3-, and 7-day precipitation extremes for current climate. The model captures well the regional patterns, with maximum return levels associated with the WCOAST,

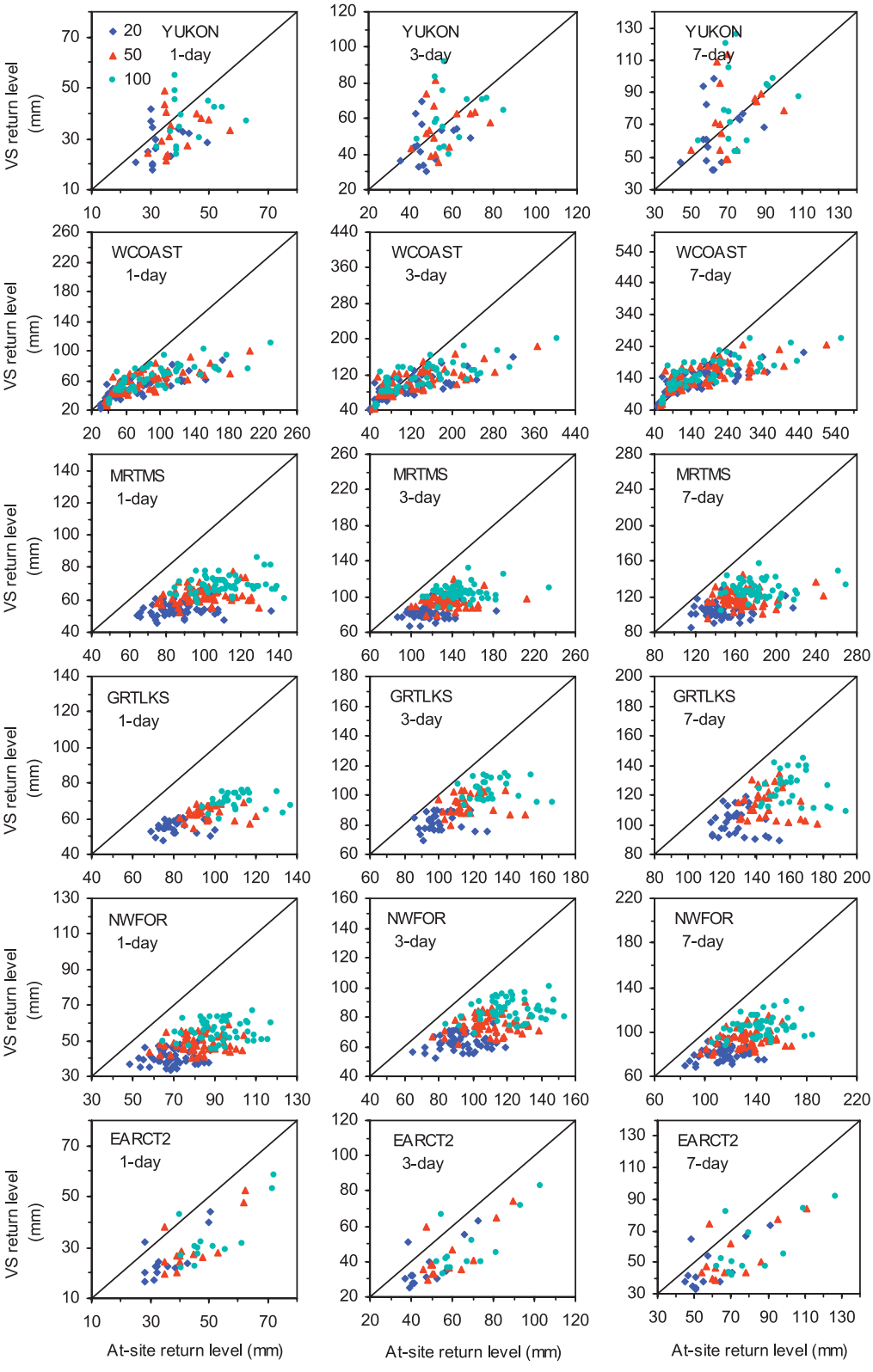

FIG. 3. Scatterplots of 20-, 50-, and 100-yr return levels of 1-, 3-, and 7-day precipitation extremes derived from observations (shown along the *x* axis) and validation simulation (VS) (shown along the *y* axis) for the current reference (1961–90) period for six selected regions.

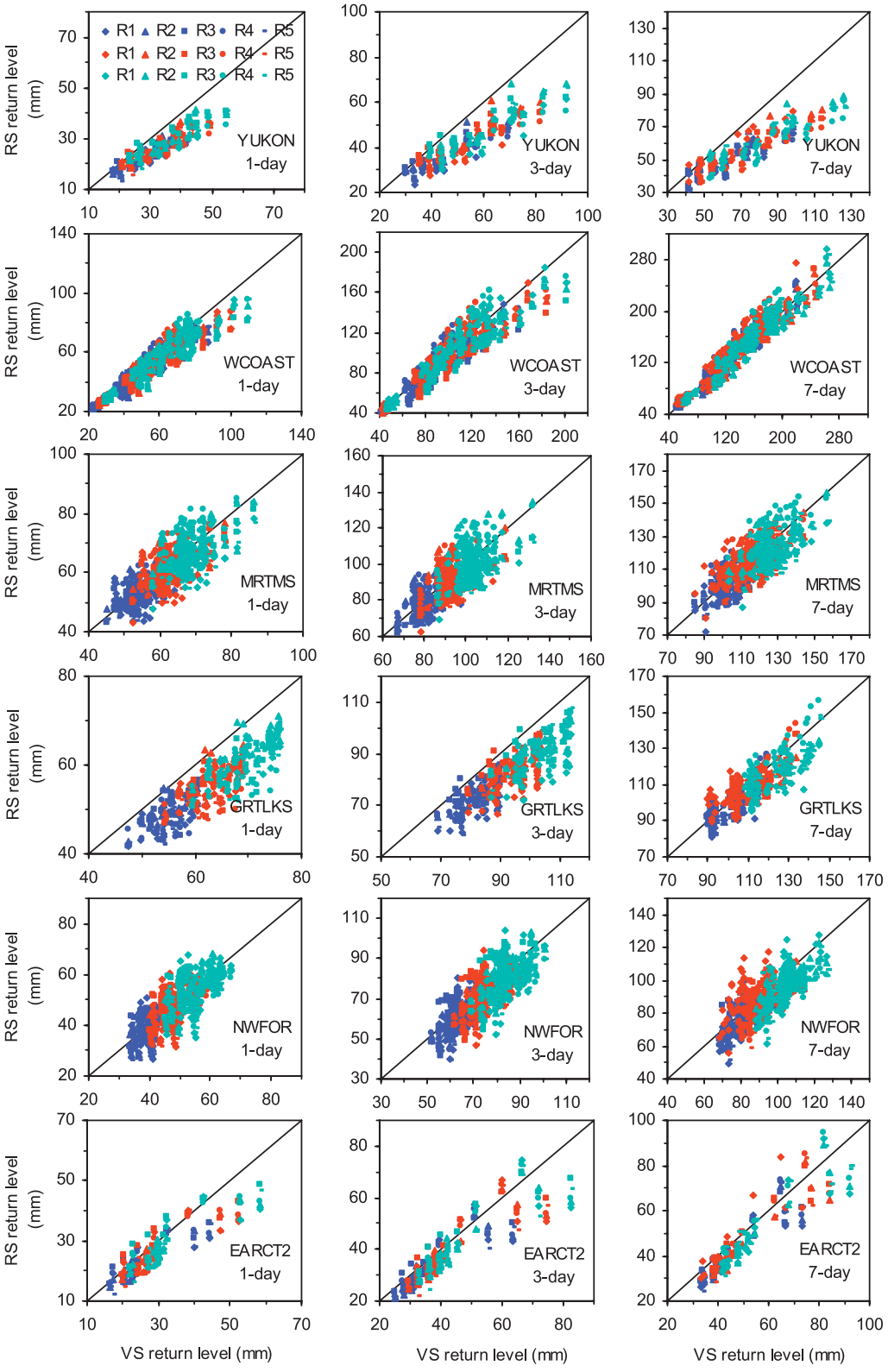

FIG. 4. Scatterplots of 20- (dark blue), 50- (red), and 100-yr (light blue) return levels of 1-, 3-, and 7-day precipitation extremes derived from the validation (shown along the *x* axis) and reference (R1–R5) simulations (shown along the *y* axis) for the current reference (1961–90) period for six selected regions.

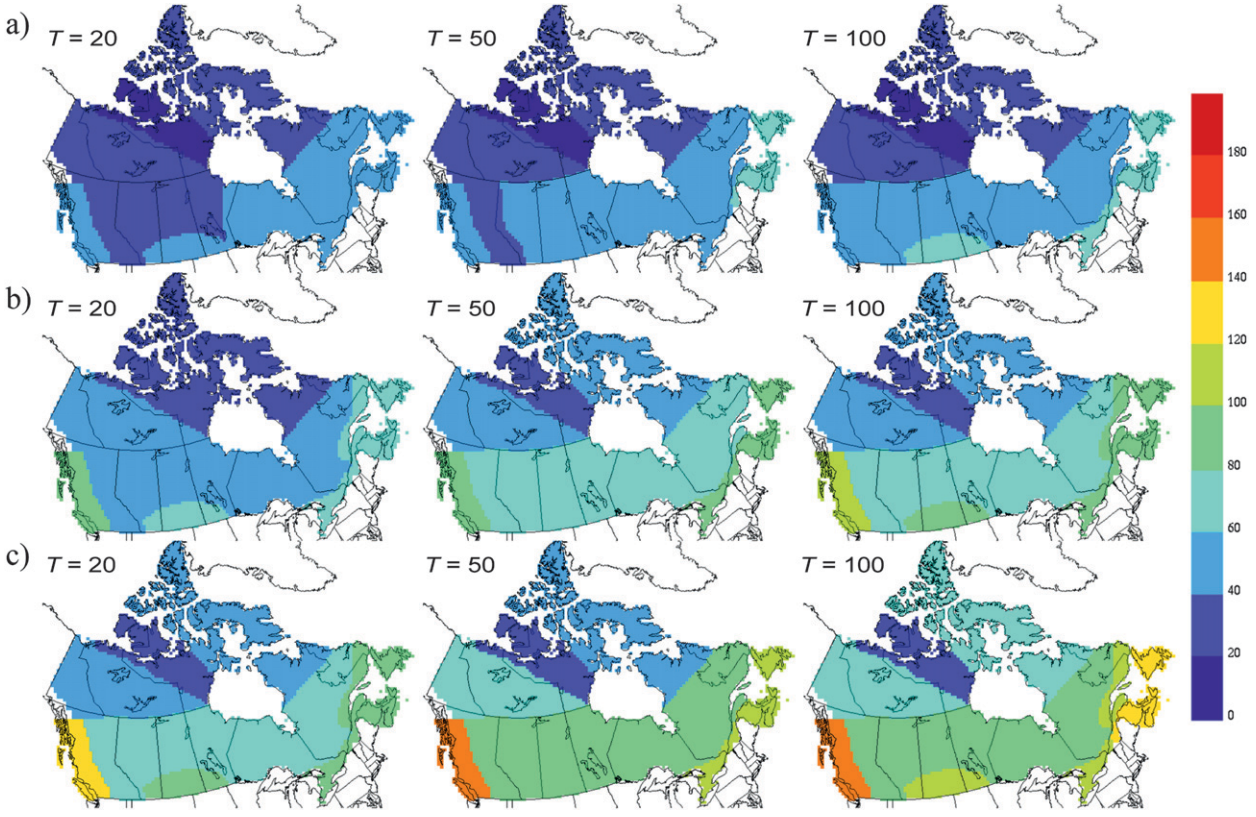

FIG. 5. Spatial distributions of (left) 20-, (middle) 50-, and (right) 100-yr regional return levels (mm) of (a) 1-, (b) 3-, and (c) 7-day precipitation extremes for the current reference (1961–90) period.

followed by the MRTMS, and the minimum values of return levels in the north. Figure 6 shows percentage projected increase/decrease in return levels at regional scale. In general, results suggest an increase in the return levels in future climate for all 12 regions, with the largest percentage increase for the northern regions. For the 20-yr return levels of 1–7-day precipitation extremes, increases in the 5%–12% range are found for GRTLKS, MRTMS, WCOAST, NWFOR, NEFOR2, and NPLNS, while larger increases in the 13%–19% range can be noticed for the northern (YUKON, MACK, EARCT1, and EARCT2) and NEFOR1 regions. The result for the WCRDRA region lies in the 11%–13% range. For the 50- and 100-yr regional return levels, the lowest percentage increase of 3%–4% and 10% is noted for 1-day extremes for MRTMS and NPLNS, respectively, and that for 7-day extremes is 6% and 9%, respectively. For the remaining regions, percentage increase lies in the 10%–20% broad range for return levels of 1–7-day precipitation extremes.

However, in absolute terms, the smallest regional level increase (3–8 mm) in the 20-yr return levels of 1–7-day precipitation extremes is found for the northern (YUKON, MACK, EARCT1, and EARCT2) and for the NWFOR, NPLNS, and MRTMS regions, while the largest increase (5–17 mm) is found for WCOAST and NEFOR1 regions. Similar patterns to the 20-yr return level are noted for the 50- and 100-yr return levels but with relatively larger magnitudes for the projected change for some regions (e.g., WCRDRA and NEFOR2).

The results of the uncertainty analysis, with $\alpha = 5\%$ using the standard error [SE(y^T)] based approach discussed in the methodology section associated with the regional changes to return levels of single- and multiday precipitation extremes are shown in Fig. 7 for six selected regions. Similar results for the test-inversion approach are shown in Fig. 8 for the same six regions. The percentage number of cases, for both single- and multiday precipitation extremes, where the confidence intervals do not overlap for the five pairs of reference and future simulations is given in Table 1. These results suggest significant increases in the regional-scale 20-yr return levels for most of the regions except MRTMS and NPLNS, where the percentage number of significant changes is not as high as for other regions. Although 50- and 100-yr return levels are projected to increase over all regions, the increases are not as strongly significant as for the 20-yr return level. It is important to mention that

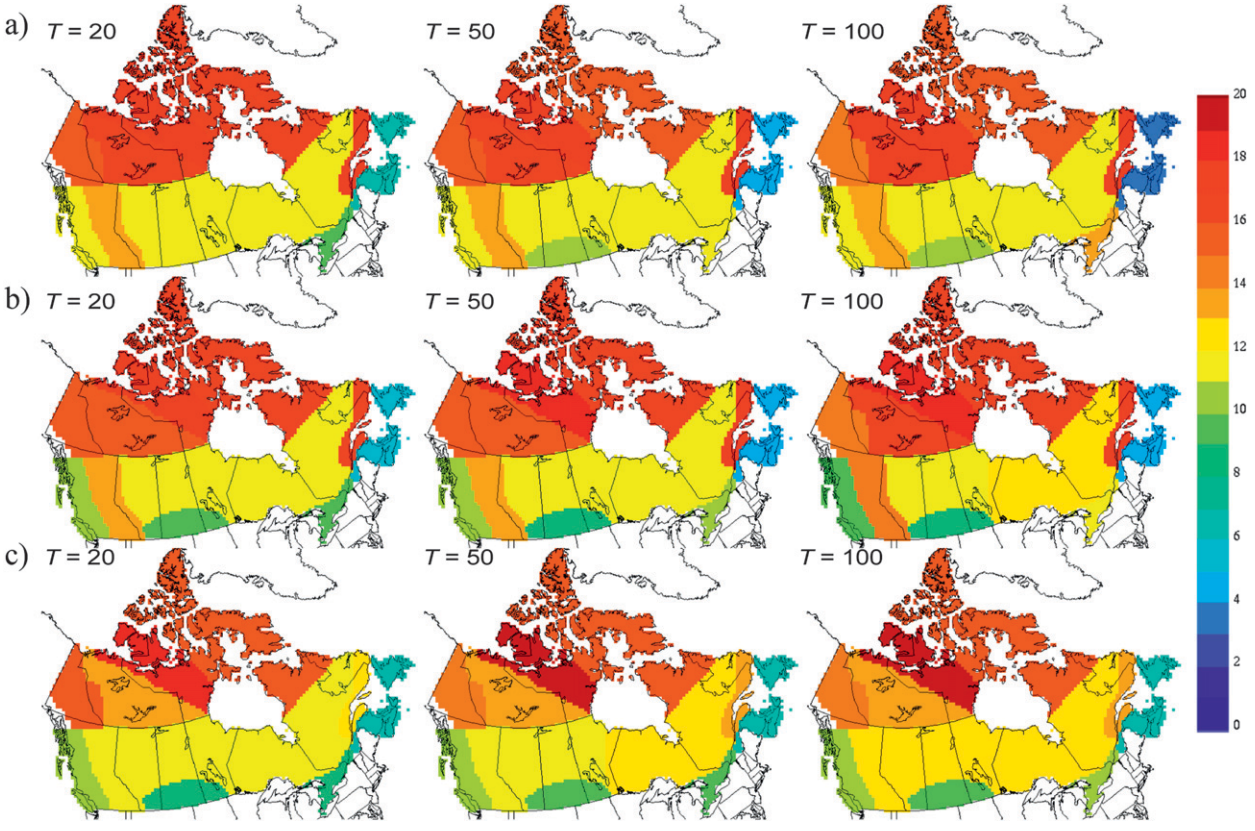

FIG. 6. Projected changes (in %) to the (left) 20-, (middle) 50-, and (right) 100-yr regional return levels of (a) 1-, (b) 3-, and (c) 7-day precipitation extremes for the future (2041–70) period with respect to the current (1961–90) reference period.

much narrower confidence intervals than the ones shown in Figs. 7 and 8 were obtained when neglecting the effects of spatial correlations, indicating that ignoring spatial dependence of CRCM gridcell-based precipitation extremes can result in underestimation of uncertainty. A summary of the uncertainty analysis at the same significance level using the test-inversion approach, which resulted in asymmetric confidence intervals, is also given in Table 1 for 20-, 50-, and 100-yr return levels. It also suggests the same conclusions as presented above for the standard error approach. However, compared to the results of the former approach, the percentage number of significant changes is slightly higher for the latter approach.

(ii) Grid-cell-level projections

The 20-, 50-, and 100-yr return levels for 1-, 3-, and 7-day precipitation extremes in current climate computed using the RFA approach and downscaled to gridcell level are shown in Fig. 9. This figure provides more detailed spatial information compared to Fig. 5 and shows larger return levels along the west coast and smaller ones for the northern regions.

The projected changes at gridcell level are shown in Fig. 10. Here, 20-, 50-, and 100-yr return levels of 1–7-day precipitation extremes increase over most of Canada, with values as high as 28% for some parts of the northern (MACK, EARCT1, and EARCT2) regions. However, some gridcells in the WCRDRA, NWFOR, NPLNS, and MRTMS show slight negative changes. Compared to areas with projected increases, the areas with negative changes, with the minimum values of −2% to −5%, are far less widespread. The spatial patterns are very similar for 20-, 50-, and 100-yr return levels.

In the following, the results of projected changes, in absolute terms, for the 20-yr return level are summarized first, followed by those for the 50- and 100-yr return levels of 1–7-day extremes. For the 20-yr return level, the projected increase varies between 4–10 mm for 1-day extremes, while that for 3- and 7-day extremes varies between 9–18 mm over the study domain. Maximum increases on the order of 16–24 mm for 3-day extremes and on the order of 18–33 mm for 7-day extremes are found for some gridcells over WCOAST, WCRDRA, and NEFOR2. Relatively smaller changes are found over northern (YUKON, MACK, EARCT1,

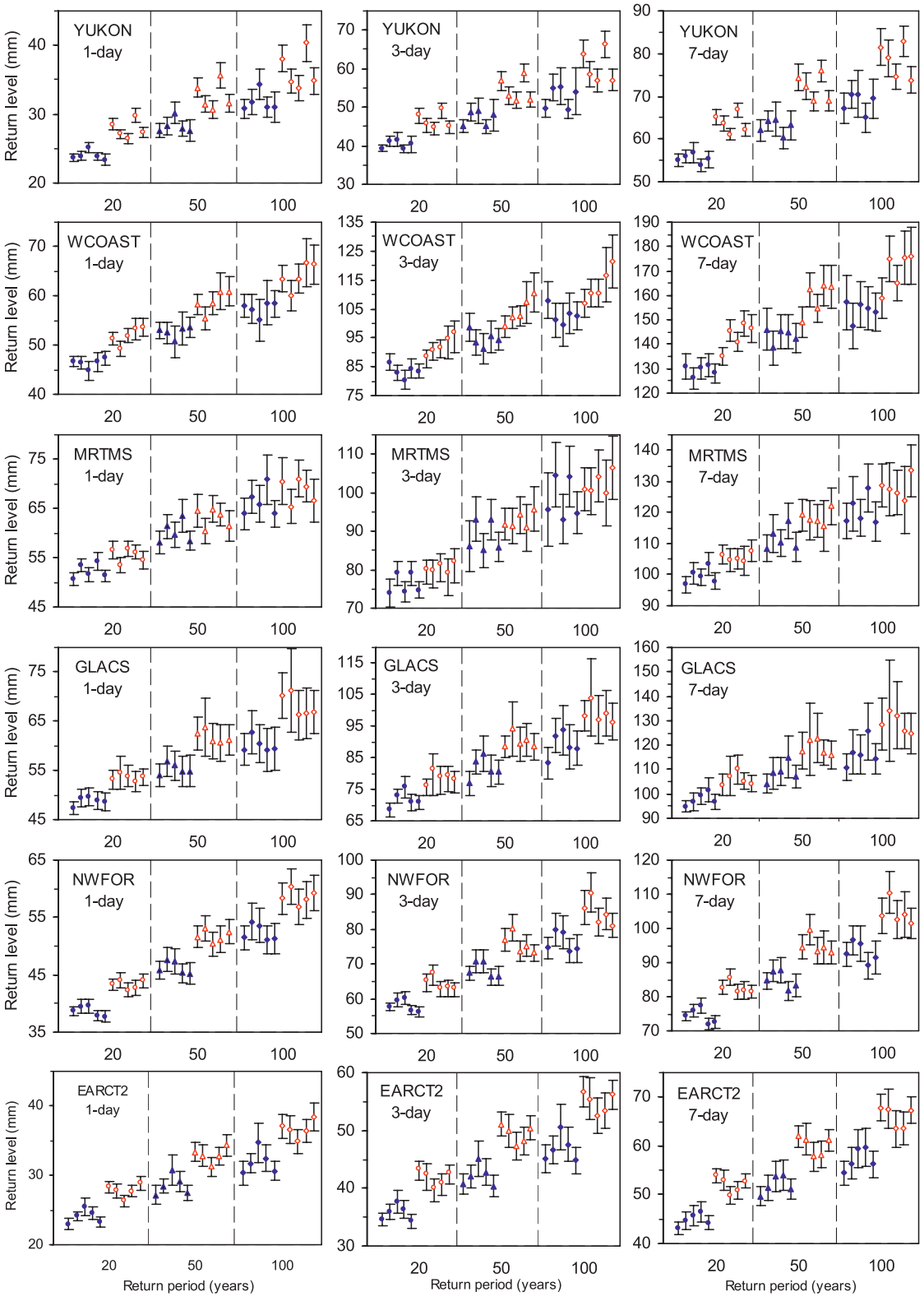

FIG. 7. Regional-scale 20-, 50-, and 100-yr return levels of 1-, 3-, and 7-day precipitation extremes for the R1–R5 (blue symbols) and F1–F5 (red symbols) simulations. Vertical bars are the 95% confidence intervals obtained using the vector bootstrap resampling approach and the standard error-based method. In each pentad, plots from left to right respectively correspond to the five current (R1–R5) and five future (F1–F5) simulations.

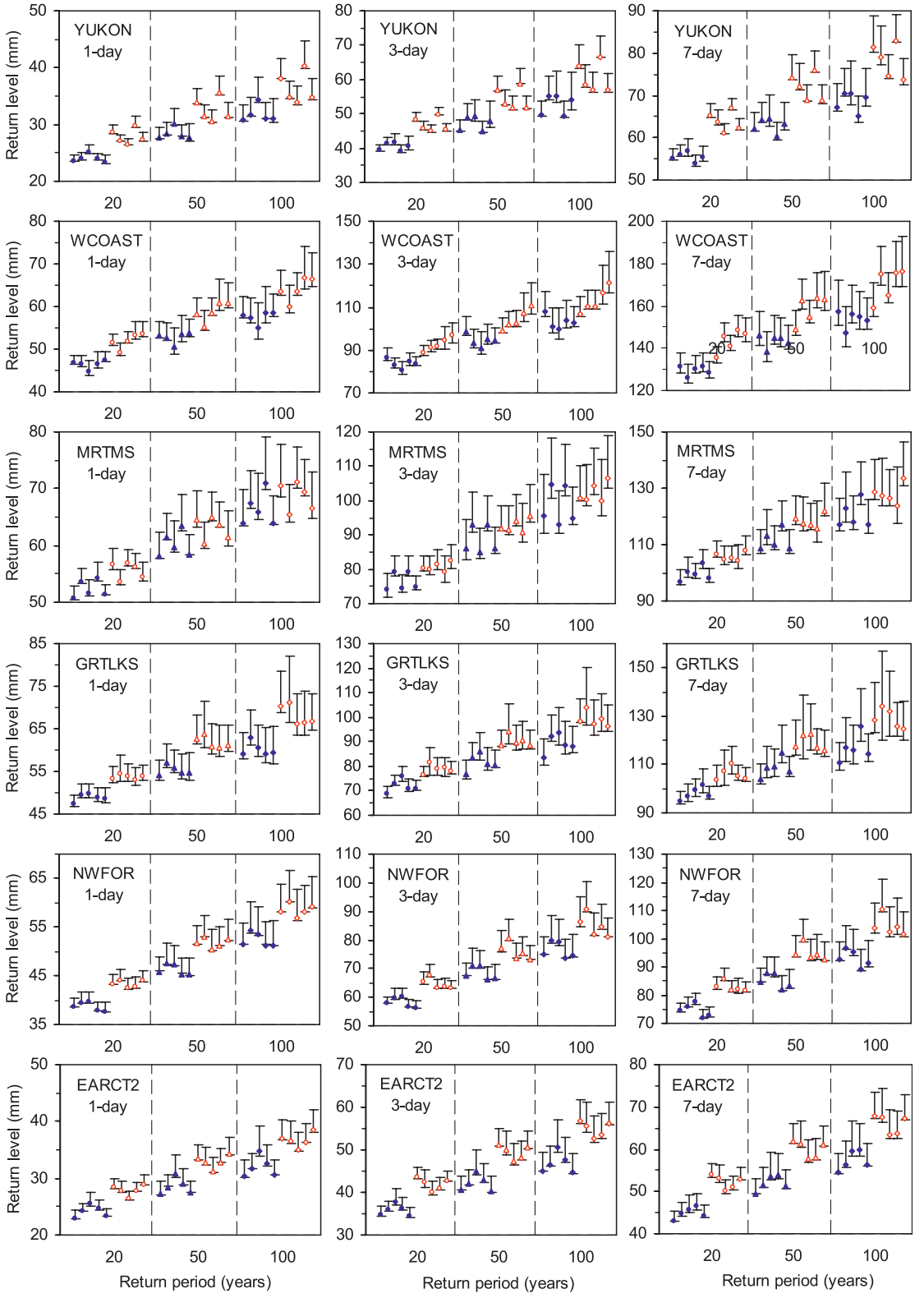

FIG. 8. Regional-scale 20-, 50-, and 100-yr return levels of 1-, 3-, and 7-day precipitation extremes for the R1–R5 (blue symbols) and F1–F5 (red symbols) simulations. Vertical bars are the 95% confidence intervals obtained using the vector bootstrap resampling approach and the test-inversion method. In each pentad, plots from left to right respectively correspond to the five current (R1–R5) and five future (F1–F5) simulations.

TABLE 1. Percentage number of 95% confidence interval comparisons wherein changes in 20-, 50-, and 100-yr regional-scale return levels of 1-, 3-, and 7-day precipitation events are found statistically significant.

	Standard error–based method			Test-inversion method		
Region	20 yr	50 yr	100 yr	20 yr	50 yr	100 yr
YUKON	93	93	67	93	93	66
WCOAST	87	80	60	87	80	60
MRTMS	53	47	20	60	53	20
GRTLKS	80	60	40	80	60	40
NWFOR	87	80	73	93	87	73
EARCT2	87	87	76	87	87	66
EARCT1	100	100	100	87	87	66
MACK	100	100	60	100	100	80
NEFOR1	93	93	67	93	93	73
NEFOR2	100	100	100	100	100	100
NPLNS	53	47	27	53	47	33
WCRDRA	100	93	80	100	93	93

and EARCT2), NWFOR, NPLNS, and MRTMS regions. As mentioned earlier, the results also suggest decrease in return levels in future climate for few gridcells located mostly in the southern part of the study domain. For 50- and 100-yr return levels of 1-day extremes, overall dominant increase in magnitude is between 3 and 10 mm, while for 7-day extremes it is between 8 and 18 mm. However, maximum increases of the order of 10–18 mm are found for some gridcells over WCOAST, NEFOR1, NEFOR2, and GRTLKS regions for 1-day extremes, and they reach up to 18–35 mm for 7-day extremes; similar behavior is noted along the southern boundary of the EARCT1 region, next to the NEFOR2 region.

2) GBA APPROACH

The GBA is implemented by fitting the GEV distribution to gridcell-based extreme precipitation extremes derived from the reference (R1–R5) and future (F1–F5) simulations. Grid-cell based ensemble averages of 20-, 50-, and 100-yr return levels for 1-, 3-, and 7-day precipitation extremes for current climate are shown in Fig. 11, and the projected changes are shown in Fig. 12. The spatial features in Fig. 11 are in general very similar to those in Fig. 9 corresponding to the regional return levels from RFA approach downscaled to the gridcell level. In the following, the results of projected changes in 20-yr return level are presented first, followed by those for the 50- and 100-yr return levels of 1- and 7-day

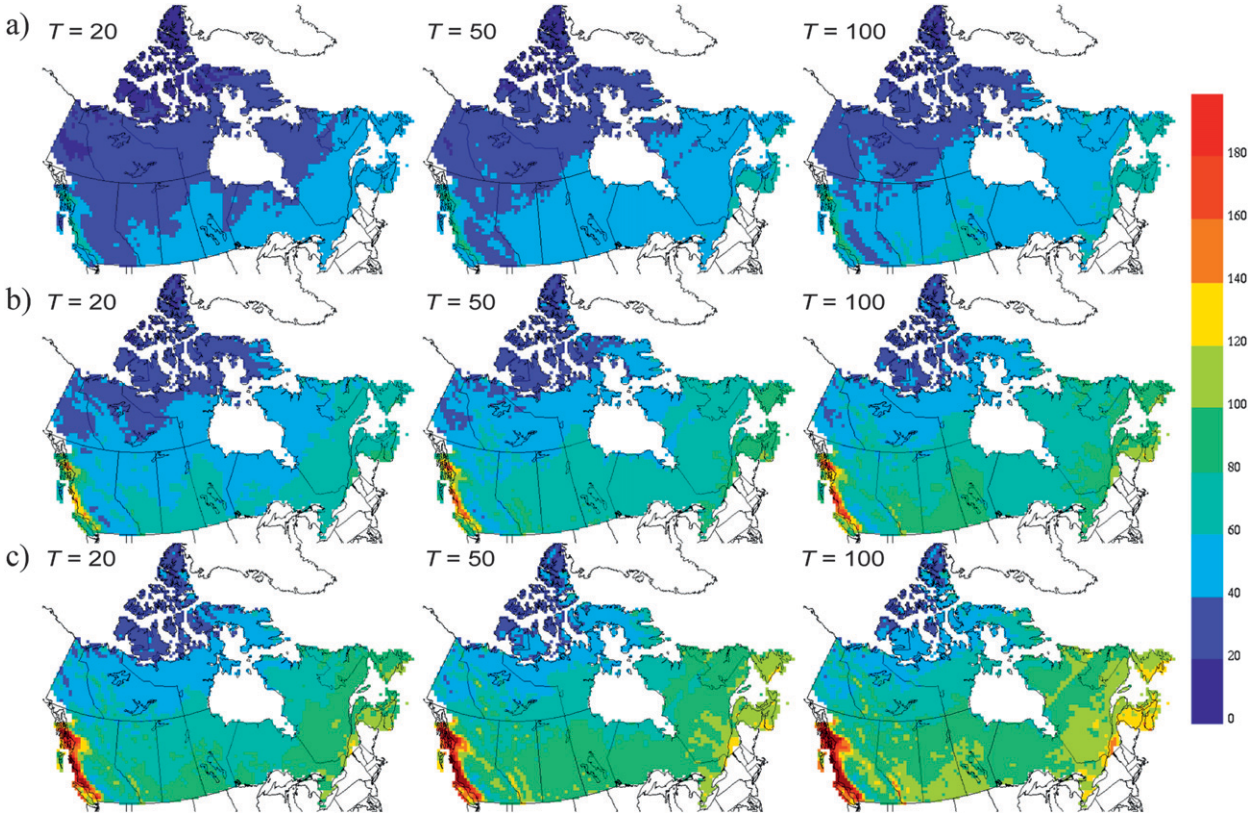

FIG. 9. Spatial distributions of (left) 20-, (middle) 50-, and (right) 100-yr return levels (in mm) of (a) 1-, (b) 3-, and (c) 7-day precipitation extremes at the CRCM gridcell level, obtained using the RFA approach, for the current reference (1961–90) period.

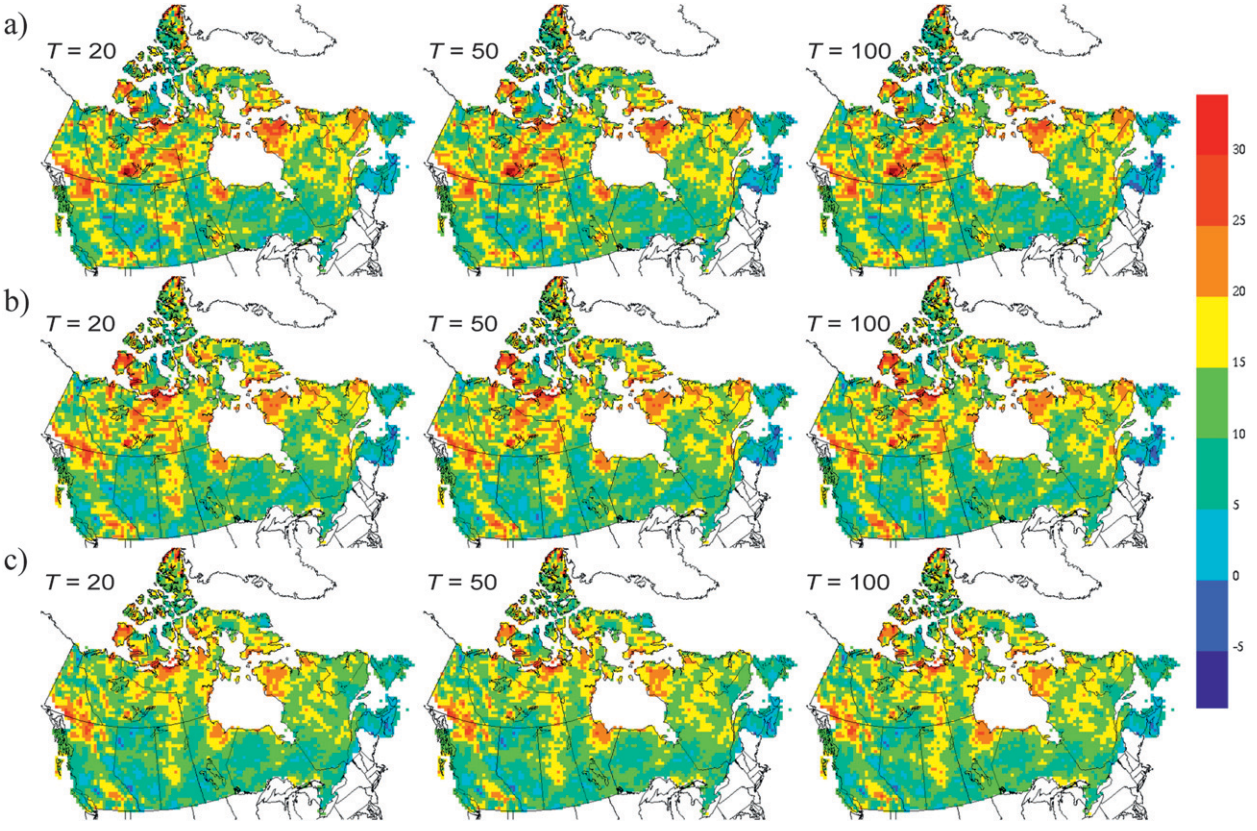

FIG. 10. Percentage change between future and reference period (left) 20-, (middle) 50-, and (right) 100-yr return levels of (a) 1-, (b) 3-, and (c) 7-day precipitation extremes, obtained using the RFA approach, at the CRCM gridcell level.

extremes only. Here, a 5%–30% increase in 20-yr return level of 1-day precipitation extremes is dominant in most of the regions. Decreases on the order of −5% to −15% are mainly present in WCRDRA, NWFOR, NPLNS, NEFOR2, and MRTMS as well as in northern regions but with smaller values of change. For 7-day precipitation extremes, areas with 21%–45% increase are seen in northern regions, northeastern part of NPLNS, and northern part of NEFOR1, while areas with decreases of −3% to −11% are concentrated in WCRDRA, NWFOR, NPLNS, and MRTMS. For the 50- and 100-yr return levels of 1-day precipitation extremes, increases are on the order of 10%–50% and 10%–60%, respectively. Distribution of decreases remains the same as for the 20-yr return level but vary from −5% to −23% for 50-yr and from −8% to −30% for 100-yr return levels. For the 50- and 100-yr return levels of 7-day extremes, 2%–20% and 5%–25% increases, respectively, are noted. Decreases from −4% to −22% for 50-yr return level and from −5% to −29% for 100-yr return level are present in NWFOR, NPLNS, NEFOR1, and MRTMS regions.

In terms of absolute changes, for 20-yr return level of 1-day extremes, changes in magnitude from 3–10 mm are found in majority of the Canadian regions. However, areas with changes up to 15 mm are found in WCOAST, eastern part of NEFOR2, NEFOR1, MRTMS, and GRTLKS. The WCRDRA, NWFOR, NPLNS, and southern MRTMS show the lowest decrease and even negative change in some areas. A similar pattern is found for extremes of longer duration but with dominant changes of 5–15 mm and 10–20 mm for 3- and 7-day extremes, respectively.

For higher return levels, the spatial distribution of increases and decreases in 1-day extremes is similar to that of the 20-yr return level but with slightly higher values for change, for example, 5–20 mm for 100-yr return level. The largest increases (up to 30 mm) are found in MACK, WCRDRA, NWFOR, NEFOR1, MRTMS, and GRTLKS. For 7-day extremes, central and western regions exhibit increases up to 32 and 73 mm for 50- and 100-yr return levels, respectively. Decreases of −1 to −20 mm are common for 7-day extremes and tend to be larger in gridboxes located in WCRDRA, NWFOR, NPLNS, NEFOR1, and MRTMS.

In general, for both the RFA and GBA approaches, the spatial distribution of projected increase/decrease is

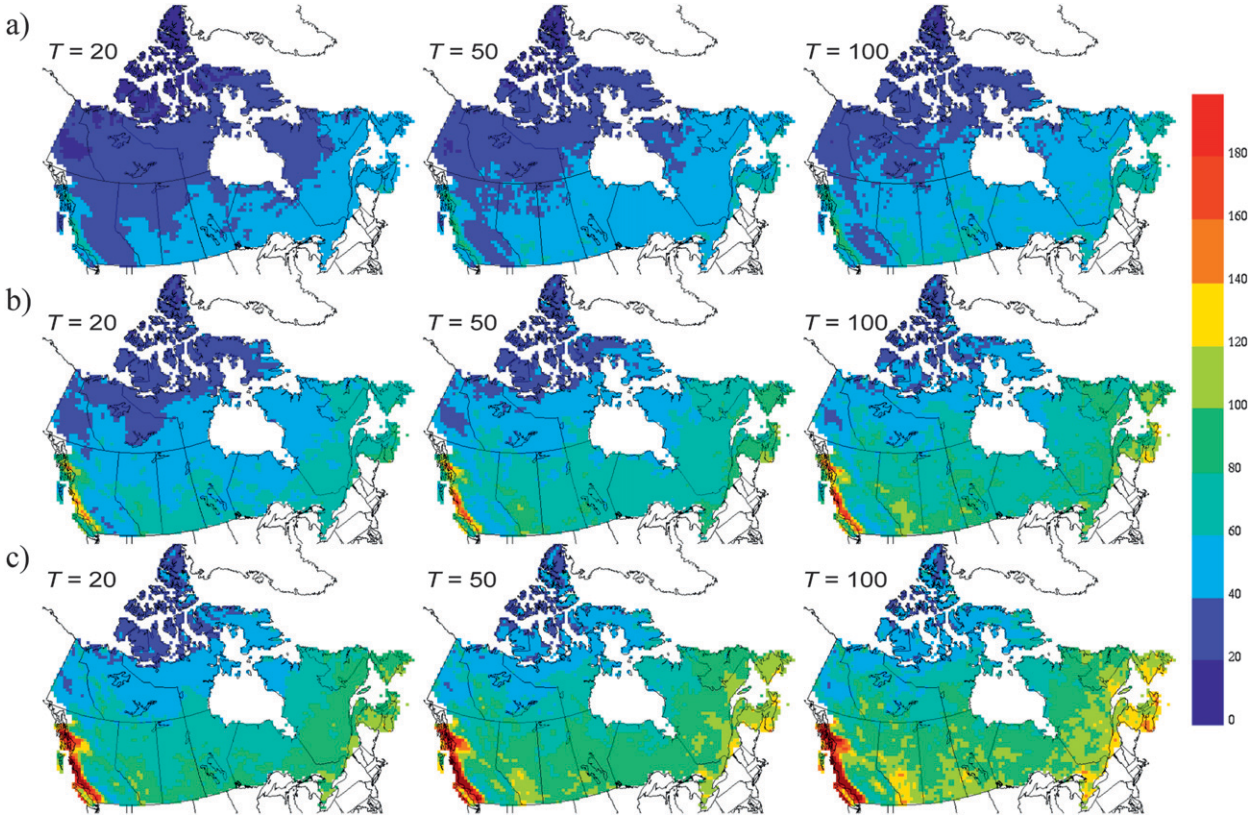

FIG. 11. Spatial distributions of ensemble averaged (left) 20-, (middle) 50-, and (right) 100-yr return levels (in mm) of (a) 1-, (b) 3-, and (c) 7-day precipitation extremes, obtained using the GBA approach, at the CRCM gridcell level for the current reference (1961–90) period.

very similar, particularly for 20-yr return period, albeit the slightly higher values for GBA. Careful analysis suggests increasing differences between the two approaches with increasing return periods. For the GBA approach for higher return periods, areas with negative changes are more widespread than for the RFA. This is not unexpected because the GBA approach, compared to the RFA, would tend to provide less reliable return levels for higher return periods because of short sample size reasons.

6. Discussion and conclusions

Evaluation of CRCM-simulated characteristics of precipitation extremes, that is, 20-, 50- and 100-yr return levels of single- and multiday (i.e., 1-, 2-, 3-, 5-, 7- and 10-day) AM (April–September) precipitation amounts, and their projected changes over Canada are studied using an ensemble of CRCM simulations and two complementary frequency analysis approaches, namely, RFA and GBA. The RFA approach involves pooling of data of homogeneous regions and can provide more reliable estimates of return values associated with longer return periods compared to GBA, which provides higher spatial information as it operates at gridcell scale. It should be noted that the information of projected changes at regional scale obtained for the RFA case can also be downscaled to gridcell level.

The CRCM simulations considered in this study include a validation simulation for the 1961–90 period, where the RCM is driven by ERA-40 at its boundaries and an additional ensemble of 10 CRCM simulations, of which five correspond to current reference (1961–90) period, while the remaining five are corresponding simulations of future (2041–70) period following the SRES A2 scenario.

In the present study, Canadian climatic regions from Plummer et al. (2006) are adopted to develop the RFA approach. Statistical homogeneity of these regions, required for the RFA approach, is verified by applying the regional homogeneity tests, devised by Hosking and Wallis (1997), to single- and multiday precipitation extremes, derived from rehabilitated precipitation dataset of Canada. It is difficult to achieve absolute homogeneity of these regions simultaneously for all single- and multiday precipitation extremes. Therefore, a climatic region is assumed homogeneous or approximately so if it passes the homogeneity tests for at least three out of six

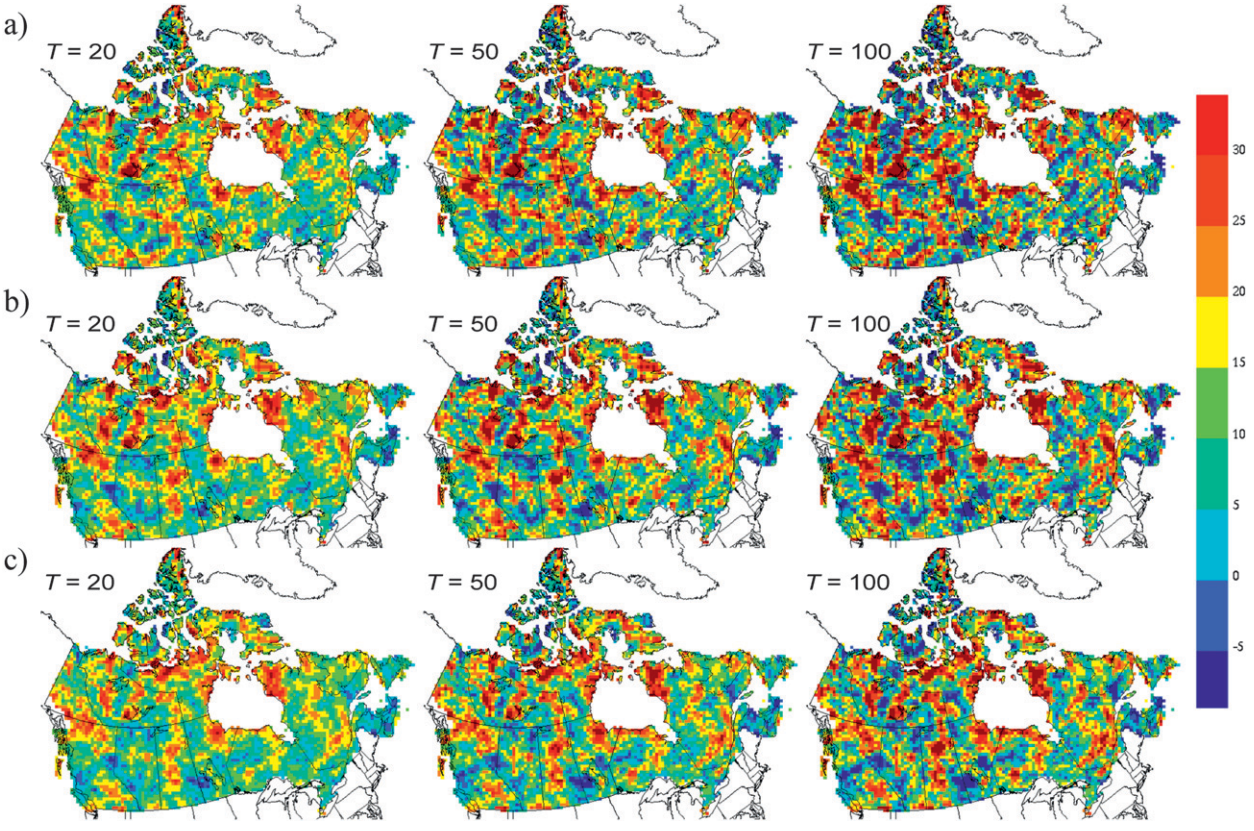

FIG. 12. Percentage change between future and reference period (left) 20-, (middle) 50-, and (right) 100-yr return levels of (a) 1-, (b) 3-, and (c) 7-day precipitation extremes, obtained using the GBA approach, at the CRCM gridcell level.

sets of single- and multiday extremes. In a similar manner, a best-fit regional distribution selected for deriving regional growth curves is the one that is found most suitable for modeling majority of the regional distributions of single- and multiday precipitation extremes. This criterion suggests that the GEV distribution, followed by GNO, is the most suitable regional distribution to model various precipitation extremes. Based on this finding, the GEV distribution was selected to implement the GBA approach. However, for the RFA approach, the identified best-fit regional distribution was used for each climatic region.

Projected changes to return levels associated with 20-, 50-, and 100-yr return periods are derived both in terms of percentage changes and in terms of absolute changes for the 2041–70 period with reference to the 1961–90 period. Concerning their usefulness for revision of design standards, either of the projected changes could be used to guide design recommendations for future infrastructure facilities; however, caution is necessary given the uncertainties. Also, note that no attempt is made to investigate the influence of multidecadal cycles on projected changes to return levels. Such studies will be considered in the future when ensembles of longer simulations spanning the 1961–2100 period will become available.

From the various analyses presented in this paper, the following main conclusions can be drawn:

1) Seven out of the 10 predefined Canadian climatic regions (YUKON, MACK, WCOAST, NWFOR, NPLNS, GRTLKS, and MRTMS) satisfy statistical homogeneity criteria required for performing RFA of single- and multiday precipitation extremes. To perform a meaningful RFA, two of the three remaining regions (EARCT and NEFOR) are divided into two subregions using the cluster analysis algorithm. However, the same algorithm did not result in useful contiguous subdivisions of the WCRDRA region and hence the results of RFA for this region could be questioned.
2) Comparison of 20-, 50-, and 100-yr return levels, derived from the validation simulation, with those derived from observed dataset suggests negative performance errors for most of the climatic regions of Canada. In a similar manner, the boundary forcing errors are assessed by comparing the same return

levels derived from the reference simulations with those of the validation simulation. In general, the boundary forcing errors are smaller compared to the performance errors.

3) On a regional basis, northern Canadian climatic regions (MACK, EARCT1, and EARCT2) exhibit the lowest absolute but highest percentage change in 20-, 50-, and 100-yr return levels of precipitation extremes. The range of absolute changes in 20-yr return levels of 1–7-day extremes is the minimum, between 3–8 mm, for northern regions, NWFOR, NPLNS, and MRTMS and maximum, between 5–13 mm, for WCOAST and NEFOR1. The projected changes in regional return levels for 20-yr return period are found more likely to be statistically significant than those for the 50- and 100-yr return periods. However, the possibility that the 30-yr sample size used in this study is not long enough to reliably estimate projected changes to return levels corresponding to large return periods cannot be ruled out.
4) The dominant range of projected changes, realized using the RFA approach, at the CRCM gridcell level is between 4–10 mm for 20-yr return level of 1-day precipitation extremes and it increases to 9–18 mm for 7-day extremes. For 50- and 100-yr return levels, this range of projected change does not vary much. Negative changes are found mostly in southern parts of the study domain for scattered gridcells, but with no coherent patterns at the regional level.
5) For the GBA approach, the dominant projected change in 20-yr return levels of 1-day precipitation extremes is between 3–10 mm and it increases to 5–15 mm and 10–20 mm for 3- and 7-day precipitation extremes, respectively. Negative changes at gridcell scale are found more often for the GBA approach than for the RFA. Areas with negative changes are present nearly in all climatic regions. Though negative changes of larger magnitude are noted, the majority of these changes lie in the range from zero to −5%.
6) The results of the projected changes, realized with the RFA and GBA approaches at the CRCM gridcell scale, are more similar for the 20-yr return period than for the 50- and 100-yr return periods, suggesting that the GBA approach suffers from small sample size uncertainties for higher return periods.
7) Concerning practical implications, it is expected that an increase in magnitude of short (i.e., 1-day) and longer (i.e., 7-day) duration precipitation extremes will have severe implications for various water resource–related development and management activities such as combined sewer systems, flood control in fast responding areas, and water storage systems, etc. The RFA approach used in this article would be particularly useful to assess projected changes at watershed scale, which are much smaller in size compared to the climatic zones considered in this analysis and therefore would exhibit higher degree of homogeneity.
8) Since uncertainties related to the choice of a regional distribution for frequency analysis of single- and multiday precipitation extremes and spatial correlations for deriving confidence intervals are taken into account when assessing significance of changes, future directions, and challenges involve appropriate apportionment of sources of uncertainty coming from scenario development and model parameterization as well as other unidentified factors. The results presented should be interpreted carefully due to the lack of high-quality observational records, particularly for the northern Canadian regions for performing validation and also due to the limitations of the CRCM. It is important to mention here that Emori et al. (2005) showed that the simulation of extreme daily precipitation can significantly depend on model parameterization. Therefore, the formulation of RCMs contributes considerably to uncertainties involved in assessment of changes to precipitation extremes. In that spirit, future improvements of model parameterization and changes in scenario development may produce different, perhaps better, estimates than the ones presented in this study. However, it is less likely that the sign of change obtained from this study will vary significantly for many parts of Canada.

Acknowledgments. This research was funded by the Canadian Foundation for Climate and Atmospheric Sciences (CFCAS), MITACS, the Ouranos Consortium, and the Pacific Climate Impacts Consortium. Thanks are due to Éva Mekis, from Atmospheric Science and Technology Directorate of Environment Canada, for help with the rehabilitated precipitation dataset. The Climate Simulations Team of the Ouranos Consortium is gratefully acknowledged for providing the daily precipitation outputs from the CRCM transient climate change simulations that are used in this study. The authors would also like to thank the anonymous referees for their useful suggestions.

REFERENCES

Anderson, C. J., and Coauthors, 2003: Hydrological processes in regional climate model simulations of the central United States flood of June–July 1993. *J. Hydrometeor.,* **4,** 584–598.

Bechtold, P., E. Bazile, F. Guichard, P. Mascart, and E. Richard, 2001: A mass flux convection scheme for regional and global models. *Quart. J. Roy. Meteor. Soc.,* **127,** 869–886.

Beniston, M., and Coauthors, 2007: Future extreme events in European climate: An exploration of regional climate model projections. *Climatic Change,* **81,** 71–95.

Booij, M. J., 2002: Extreme daily precipitation in western Europe with climate change at appropriate spatial scales. *Int. J. Climatol.,* **22,** 69–85.

Burn, D. H., 2003: The use of resampling for estimating confidence intervals for single site and pooled frequency analysis. *Hydrol. Sci. J.,* **48,** 25–38.

Carpenter, J., 1999: Test inversion bootstrap confidence intervals. *J. Roy. Stat. Soc.,* **B61,** 159–172.

Caya, D., and R. Laprise, 1999: A semi-implicit semi-Lagrangian regional climate model: The Canadian RCM. *Mon. Wea. Rev.,* **127,** 341–362.

Cunnane, C., 1989: Statistical distributions for flood frequency analysis. WMO Rep. 718, WMP, 73 pp.

Davison, A. C., and D. V. Hinkley, 1997: *Bootstrap Methods and Their Application*. Cambridge University Press, 582 pp.

Efron, B., and R. J. Tibshirani, 1993: *An Introduction to the Bootstrap*. Chapman and Hall, 436 pp.

Ekström, M., H. J. Fowler, C. G. Kilsby, and P. D. Jones, 2005: New estimates of future changes in extreme rainfall across the UK using regional climate model integrations. 2. Future estimates and use in impact studies. *J. Hydrol.,* **300,** 234–251.

Emori, S., A. Hasegawa, T. Suzuki, and K. Dairaku, 2005: Validation, parameterization dependence and future projection of daily precipitation simulated with a high-resolution atmospheric GCM. *Geophys. Res. Lett.,* **32,** L06708, doi:10.1029/2004GL022306.

Faulkner, D. S., and D. A. Jones, 1999: The FORGEX method of rainfall growth estimation, III. Examples and confidence intervals. *Hydrol. Earth Syst. Sci.,* **3,** 205–212.

Fowler, H. J., M. Ekström, C. G. Kilsby, and P. D. Jones, 2005: New estimates of future changes in extreme rainfall across the UK using regional climate model integrations. 1: Assessment of control climate. *J. Hydrol.,* **300,** 212–233.

Frei, C., J. H. Christensen, M. Déqué, D. Jacob, R. G. Jones, and P. L. Vidale, 2003: Daily precipitation statistics in regional climate models: Evaluation and intercomparison for the European Alps. *J. Geophys. Res.,* **108,** 4124, doi:10.1029/2002JD002287.

——, R. Schöoll, S. Fukutome, J. Schmidli, and P. L. Vidale, 2006: Future change of precipitation extremes in Europe: Intercomparison of scenarios from regional climate models. *J. Geophys. Res.,* **111,** D06105, doi:10.1029/2005JD005965.

GREHYS, 1996: Presentation and review of some methods for regional flood frequency analysis. *J. Hydrol.,* **186,** 63–84.

Hall, M. J., H. F. P. van den Boogaard, R. C. Fernando, and A. E. Mynett, 2004: The construction of confidence intervals for frequency analysis using resampling techniques. *Hydrol. Earth Syst. Sci.,* **8,** 235–246.

Hosking, J. R. M., and J. R. Wallis, 1997: *Regional Frequency Analysis*. Cambridge University Press, 224 pp.

Houghton, J. T., and Coauthors, 2001: *Climate Change 2001: The Scientific Basis*. Cambridge University Press, 881 pp.

Kain, J. S., and J. M. Fritsch, 1990: A one-dimensional entraining/detraining plume model and its implication in convective parameterization. *J. Atmos. Sci.,* **47,** 2784–2802.

Khaliq, M. N., T. B. M. J. Ouarda, L. Sushama, and P. Gachon, 2009: Identification of hydrological trends in the presence of serial and cross correlations: A review of selected methods and their application to annual flow regimes of Canadian rivers. *J. Hydrol.,* **368,** 117–130.

Kharin, V. V., and F. W. Zwiers, 2000: Changes in the extremes in an ensemble of transient climate simulations with a coupled atmosphere ocean GCM. *J. Climate,* **13,** 3760–3788.

Kiktev, D., D. M. H. Sexton, L. Alexander, and C. K. Folland, 2003: Comparison of modeled and observed trends in indices of daily climate extremes. *J. Climate,* **16,** 3560–3571.

——, ——, ——, and ——, 2004: Corrigendum: Comparison of modeled and observed trends in indices of daily climate extremes. *J. Climate,* **17,** 2489.

Laprise, R., D. Caya, A. Frigon, and D. Paquin, 2003: Current and perturbed climate as simulated by the second-generation Canadian Regional Climate Model (CRCM-II) over northwestern North America. *Climate Dyn.,* **21,** 405–421.

Mailhot, A., S. Duchesne, D. Caya, and G. Talbot, 2007: Assessment of future change in intensity–duration–frequency (IDF) curves for Southern Quebec using the Canadian Regional Climate Model (CRCM). *J. Hydrol.,* **347,** 197–210.

May, W., 2008: Potential future changes in the characteristics of daily precipitation in Europe simulated by the HIRHAM regional climate model. *Climate Dyn.,* **30,** 581–603.

McFarlane, N. A., J. F. Scinocca, M. Lazare, R. Harvey, D. Verseghy, and J. Li, 2005: The CCCma third generation atmospheric general circulation model. Rapport interne du Centre Canadien de la Mod'elisation et de l'Analyse Climatique, 25 pp. [Available online at http://www.cccma.ec.gc.ca/papers/jscinocca/AGCM3_report.pdf.]

Mekis, É., and W. D. Hogg, 1999: Rehabilitation and analysis of Canadian daily precipitation time series. *Atmos.–Ocean,* **37,** 53–85.

Osborn, T. J., and M. Hulme, 1997: Development of a relationship between station and grid-box rainday frequencies for climate model evaluation. *J. Climate,* **10,** 1885–1908.

Palmer, T. N., and J. Räisänen, 2002: Quantifying the risk of extreme seasonal precipitation events in a changing climate. *Nature,* **415,** 512–514.

Plummer, D. A., and Coauthors, 2006: Climate and climate change over North America as simulated by the Canadian RCM. *J. Climate,* **19,** 3112–3132.

Scinocca, J. F., and N. A. McFarlane, 2004: The variability of modeled tropical precipitation. *J. Atmos. Sci.,* **61,** 1993–2015.

Semmler, T., and D. Jacob, 2004: Modeling extreme precipitation events–A climate change simulation for Europe. *Global Planet. Change,* **44,** 119–127.

Sushama, L., R. Laprise, D. Caya, A. Frigon, and M. Slivitzky, 2006: Canadian RCM projected climate-change signal and its sensitivity to model errors. *Int. J. Climatol.,* **26,** 2141–2159.

——, M. N. Khaliq, and R. Laprise, 2010: Dry spell characteristics over Canada in a changing climate as simulated by the Canadian RCM. *Global Planet. Change,* **74,** 1–14.

Uppala, S. M., and Coauthors, 2005: The ERA-40 Re-Analysis. *Quart. J. Roy. Meteor. Soc.,* **131,** 2961–3012.

Verseghy, D. L., N. A. McFarlane, and M. Lazare, 1993: A Canadian land surface scheme for GCMs: II. Vegetation model and coupled runs. *Int. J. Climatol.,* **13,** 347–370.

Vincent, L. A., and E. Mekis, 2009: Discontinuities due to joining precipitation station observations in Canada. *J. Appl. Meteor. Climatol.,* **48,** 156–166.

Voss, R., W. May, and E. Roeckner, 2002: Enhanced resolution modeling study on anthropogenic climate change: Changes in extremes of the hydrological cycle. *Int. J. Climatol.,* **22,** 755–777.

Wehner, M. F., 2004: Predicted twenty-first-century changes in seasonal extreme precipitation events in the parallel climate model. *J. Climate,* **17,** 4281–4290.

Zwiers, F. W., and V. V. Kharin, 1998: Changes in the extremes of the climate simulated by CCC GCM2 under CO_2 doubling. *J. Climate,* **11,** 2200–2222.